Expression and Activity of Mutants of Fasciculin, a Peptidic Acetylcholinesterase Inhibitor from Mamba Venom*

P. Marchot, Claudine Prowse, Joan Kanter, Shelley Camp, Elizabeth Ackermann, Zoran Radić, Pierre Bougis, Palmer Taylor

Expression and Activity of Mutants of Fasciculin, a Peptidic Acetylcholinesterase Inhibitor from Mamba Venom*

Pascale Marchot‡§, Claudine N. Prowse‡, Joan Kanter‡, Shelley Camp‡, Elizabeth J. Ackermann‡, Zoran Radić‡, Pierre E. Bougis§, and Palmer Taylor‡¶

From the ‡Department of Pharmacology, University of California at San Diego, La Jolla, California 92093-0636 and §CNRS, Unité de Recherche Associée 1455, Institut Fédératif de Recherche Jean Roche, Université de la Méditeranée, Faculté de Médecine Secteur Nord, 13916 Marseille Cedex 20, France

Fasciculin, a selective peptidic inhibitor of acetylcholinesterase, is a member of the three-fingered peptide toxin superfamily isolated from snake venoms. The availability of a crystal structure of a fasciculin 2 (Fas2)-acetylcholinesterase complex affords an opportunity to examine in detail the interaction of this toxin with its target site. To this end, we constructed a synthetic fasciculin gene with an appropriate leader peptide for expression and secretion from mammalian cells. Recombinant wild-type Fas2, expressed and amplified in Chinese hamster ovary cells, was purified to homogeneity and found to be identical in composition and biological activities to the venom-derived toxin. Sixteen mutations at positions where the crystal structure of the complex indicates a significant interfacial contact point or determinant of conformation were generated. Two mutants of loop I, T8A/T9A and R11Q, ten mutants of the longest loop II, R24T, K25L, R27W, R28D, H29D, ΔPro³⁰, P31R, K32G, M33A, and V34A/L35A, and two mutants of loop III, D45K and K51S, were expressed transiently in human embryonic kidney cells. Inhibitory potencies of the Fas2 mutants toward mouse AChE were established, based on titration of the mutants with a polyclonal anti-Fas2 serum. The Arg²⁷, Pro³⁰, and Pro³¹ mutants each lost two or more orders of magnitude in Fas2 activity, suggesting that this subset of three residues, at the tip of loop II, dominates the loop conformation and interaction of Fas2 with the enzyme. The Arg²⁴, Lys³², and Met³³ mutants lost about one order of magnitude, suggesting that these residues make moderate contributions to the strength of the complex, whereas the Lys²⁵, Arg²⁸, Val³⁴-Leu³⁵, Asp⁴⁵, and Lys⁵¹ mutants appeared as active as Fas2. The Thr⁸-Thr⁹, Arg¹¹, and His²⁹ mutants showed greater ratios of inhibitory activity to immunochemical titer than Fas2. This may reflect immunodominant determinants in these regions or intramolecular rearrangements in conformation that enhance the interaction. Of the many Fas2 residues that lie at the interface with acetylcholinesterase, only a few appear to provide substantial energetic contributions to the high affinity of the complex.

Fasciculins, selective inhibitors of acetylcholinesterase

(AChE),[1] but not butyrylcholinesterase, are 7-kDa peptides with four disulfide bridges isolated from mamba venoms. They belong to the family of three-fingered snake toxins that includes the selective nicotinic receptor blockers, α-neurotoxins (1–3) and κ-neurotoxins (4, 5), the subtype-specific muscarinic receptor agonists (6, 7), the L-type calcium channel blockers, calciseptine and FS2 (8, 9), the GPIIb-IIIa antagonist and platelet aggregation inhibitor, RGD-containing dendroaspin (or mambin) (10, 11), and the cell membrane lytic cardiotoxins (or cytotoxins) (12, 13). Despite a highly conserved structural motif, the toxins in this family are directed to diverse targets, yet their individual modes of action are highly selective. The three-finger scaffold, that is also found in proteins isolated from sources other than snake venoms and devoid of toxic activity (14–17), constitutes a structural motif which accomplishes a plethora of precise, but eclectic, functions.

Fasciculins selectively inhibit mammalian and electric fish AChEs with K_i values in the pico- to nanomolar range (18–22). Several kinetic studies have shown that the fasciculin-AChE complex, despite its high affinity and extremely slow rate of dissociation, possesses residual catalytic activity (20, 23–26): in the complex, both substrate and catalytic site inhibitors are able to access the active center of the enzyme, located at the bottom of a deep and narrow gorge (27). On the other hand, fasciculin is competitive with propidium (18, 20, 24), a peripheral site inhibitor of AChE (28) which binds at an allosteric site presumed to be at the rim of the gorge (cf. Ref. 29). Three aromatic residues, that lie at the gorge rim, were found to be critical for fasciculin binding to AChE by site-directed mutagenesis of the enzyme (21).

The recently solved x-ray structures of the Fas2-mouse AChE and Fas2-Torpedo AChE complexes revealed that three domains of Fas2 anchor it to the enzyme, and delineated a large contact area consistent with the low dissociation constant of the complex; the Fas2 and AChE residues participating in the binding interface were unambiguously established, and major hydrophobic interactions were identified (30, 31). The structural analyses, however, did not reveal to what extent each contact between Fas2 and AChE contributes to the overall binding energy. In addition, the central loop of Fas2 was found to fit snugly at the gorge entrance so that the entry of other molecules, even as small as water, should be precluded. The mode of inhibition of fasciculin therefore appeared to be total

---

[1] The abbreviations used are: AChE, acetylcholinesterase; BSA, bovine serum albumin; CHO, Chinese hamster ovary; CPK, Corey-Pauling-Koltun; Fas2, natural venom-derived fasciculin 2; FPLC, fast pressure liquid chromatography; HEK, human embryonic kidney; mAChE, recombinant acetylcholinesterase from mouse; NH₄Ac, ammonium acetate; PAGE, polyacrylamide gel electrophoresis; rFas2, recombinant wild-type fasciculin 2; RIA, radioimmunoassay.

This paper is available on line at http://www-jbc.stanford.edu/jbc/

occlusion of substrate entry at the mouth of the active-site gorge. To reconcile the disparity in the kinetic and structural data, either a second portal for entry of substrate and catalytic site inhibitors in the complex or a conformational change in the enzyme, not obvious in the crystal structure, opening a gap between the gorge wall and the bound peptide, have been proposed (30).

Complete understanding of the chemistry of the Fas2-AChE association requires a functional map of the binding surfaces. By site-directed mutagenesis of a synthetic Fas2 gene, we have generated new probes aimed at analyzing the individual contributions of the fasciculin residues to complex formation and conformation. In a mammalian system, we expressed a fully processed recombinant fasciculin, rFas2, that is undistinguishable from the natural, venom-derived Fas2. Fourteen mutants, encompassing 16 amino acid residues distributed among the three loops (fingers) of Fas2, were designed based on both the kinetic and structural data. We show that common determinants are identified by the structural and the mutagenesis approaches, but only a few of the many Fas2 residues residing at the binding interface provide the critical contacts required for enzyme inhibition.

EXPERIMENTAL PROCEDURES

Materials—HEK-293 and CHO-K1 cells were obtained from American Type Culture Collection. Ultraculture and serum-free Ultra-CHO cell culture media were from BioWhittaker, and serum-free Dulbecco's modified Eagle's cell culture medium from Life Technologies, Inc. L-Methionine sulfoximine, polyethylene glycol 8000, protease-free BSA, 5,5'-dithiobis-(2-nitrobenzoic acid), acetylthiocholine iodide, and the gel-filtration molecular weight markers (Mw-GF-70 Kit) were products of Sigma. The prepacked FPLC columns, Mono S HR 5/5 and Superose-12 HR 10/30, were from Pharmacia Biotech Inc. Dialysis tubing (Spectra/Pore6) was from Spectrum Medical Industries. The BCA kit for protein assays was from Pierce. Prestained protein molecular weight standards for SDS-PAGE were from Life Technologies, Inc. ^{125}I-Na (2100 Ci mmol^{-1}) was from Amersham. Complete and incomplete Freund's adjuvants were from Difco Laboratories. Normal rabbit serum and goat anti-rabbit whole serum were from Jackson ImmunoResearch Laboratories. All buffers were made with deionized water from a Millipore MilliRO/MilliQ system.

Biological Materials—The pGS expression vector was a gift from Scios Nova Inc. (Mountain View, CA). Purification of Fas2 from *Dendroaspis angusticeps* venom has been described previously (32). Concentrations of stock solutions were determined from their UV spectra ($\epsilon_{276\ nm} = 4900\ M^{-1}\ cm^{-1}$). Wild-type AChE from mouse recombinant DNA was expressed, concentrated, and titrated as described previously (33, 34). The polyclonal anti-Fas2 serum was obtained by immunization of a Blanc du Bouscat Evic rabbit with subcutaneous multi-site injections of purified Fas2 (100–150 μg). Primary and booster injections were made with complete and incomplete Freund's adjuvants, respectively (35).

Design of Synthetic Genes Encoding Wild-type and Mutant Fas2—A cDNA encoding rFas2 and the leader peptide from erabutoxin a (36) was synthesized as two sets of complementary oligonucleotides of ~130 base pairs in length, that were annealed, ligated together, and cloned into the expression vector pGS. rFas2 was expressed from the cytomegalovirus promoter while glutamine synthetase under the control of the Rous sarcomal virus-long terminal repeat was used as a dominant selectable marker conferring resistance to a low level of methionine sulfoximine. The pGS-rFas2 plasmid was transfected into CHO-K1 cells by calcium phosphate co-precipitation with glycerol shock. Individual cell colonies which successfully integrated the rFas2 and adjacent GS genes were selected in glutamine-free Ultraculture medium in the presence of 25 μM methionine sulfoximine and grown to confluence. Clones which produced the highest Fas2 activity were then further amplified using either 250 μM or 500 μM methionine sulfoximine.

Mutagenic oligonucleotides (usually 18 mers) were used in generating Fas2 mutants according to Kunkel *et al.* (37). Mutations were done on either M13 or single-stranded pBluescript templates. The entire nucleotide sequences of the mutated plasmids were verified using dideoxy sequencing. Transient transfections into HEK-293 cells employed the pGS plasmid and coprecipitation with calcium phosphate and glycerol shock. To ascertain transfection efficiencies, 5 μg of a pcDNA-3 expression vector containing the *Escherichia coli lacZ* gene were cotransfected (38). The cells were rinsed and placed in serum-free medium 24 h after transfection. Secreted fasciculin activity was examined 48 to 72 h later.

Chromatography—Ultraculture medium containing the expressed rFas2 (10 ml/10-cm plate) was harvested every 3–4 days, centrifuged (4 °C, 10 min) to remove cell debris, extensively dialyzed against 50 mM NH$_4$Ac, pH 7.5, 0.01% (w/v) NaN$_3$, and filtered through 0.22-μm cellulose acetate filters. rFas2 was purified by cation-exchange and size-exclusion FPLC (Pharmacia) performed at 4 °C in NH$_4$Ac, pH 7.5, with flow rates of 0.5 ml min^{-1}. The dialyzed and filtered cell culture medium (up to 500 ml) was loaded on a Mono S column previously equilibrated with 50 mM NH$_4$Ac, then the column was washed extensively with the same buffer. Elution of the rFas2 fraction was performed with a 50–200 mM NH$_4$Ac gradient over 60 min, followed by an isocratic step at 200 mM NH$_4$Ac. The eluted rFas2 fraction was lyophilized, redissolved in 100 mM NH$_4$Ac, and loaded as a 200-μl sample on a Superose-12 column equilibrated in 100 mM NH$_4$Ac. For the final cation-exchange step, the pooled rFas2-containing fractions emerging from successive gel filtrations were diluted twice and loaded on the Mono S column equilibrated in 50 mM NH$_4$Ac. Elution of rFas2 was performed under isocratic conditions with 100 mM NH$_4$Ac.

All Fas2 mutants were concentrated and partially purified from the culture medium through the first ion-exchange step, then further concentrated by ultrafiltration. To prevent cross-contamination, separate Mono S columns were used for rFas2 and the Fas2 mutants, and the columns were fully regenerated after each use.

Electrophoresis—SDS-PAGE under reducing conditions used the discontinuous system of Laemmli (39) with a 20% resolving/5% stacking gel. Samples were denatured in 500 mM Tris-HCl, pH 6.8, in the presence of 5% (v/v) β-mercaptoethanol and 4% SDS, at 90 °C for 2 min, then loaded onto the gel in the presence of 10% (v/v) glycerol and 0.01% bromphenol blue. Isoelectric focusing was performed with pH 3–10 precast gels (Novex) as specified by the manufacturer. Staining was by silver nitrate.

Peptide Analyses—Amino acid analysis of rFas2 (5 nmol), previously hydrolyzed with 6 M HCl and 1% (w/v) phenol for 20 h *in vacuo*, was carried out on a ABS Auto Analyzer. Automated Edman analysis of rFas2 (250 pmol) was conducted on a ABS sequenator. Equivalent samples of venom-derived Fas2 were analyzed in parallel.

Liquid-phase Radioimmunoassay (RIA)—Lactoperoxidase-catalyzed radioiodination of Fas2 to a specific radioactivity of ~1200 Ci mmol^{-1} has been detailed elsewhere (20). The titer of the anti-Fas2 serum, defined as the serum dilution which binds 50% of the ^{125}I-Fas2 added to the sample, was determined as a 316,000-fold dilution. For standard RIAs, ^{125}I-Fas2 (10,000 cpm) was incubated at 37 °C for 90 min with the anti-Fas2 serum at its titer in 200 μl of 50 mM NaH$_2$PO$_4$/Na$_2$HPO$_4$, pH 7.5, 0.1 mg ml^{-1} BSA, and then the samples were diluted with buffer to 500 μl and incubated overnight at 4 °C. Double immunoprecipitation of the antigen-antibody complexes was performed at 4 °C with successive additions of normal rabbit serum (50 μl of a 1/50 dilution), goat anti-rabbit serum (50 μl of a 1/20 dilution), and polyethylene glycol (400 μl of a 20% (w/v) solution). Samples were centrifuged (10,000 × g, 25 min, 4 °C), and the radioactivity of the pellets was determined. Titration of the unlabeled rFas2 and Fas2 mutants by RIA was based on competition with ^{125}I-Fas2 for complexation with anti-Fas2 serum and comparison to a Fas2 standard curve.

Assay for AChE Inhibition—Relative AChE activities (40) were recorded at room temperature by microtitration on a V_{max} kinetic microplate reader (Molecular Devices Corp.) at 405 nm, in the presence of 0.5 mM acetylthiocholine iodide and 0.3 mM 5,5'-dithiobis-(2-nitrobenzoic acid), in 50 mM NaPO$_4$ buffer, pH 8.0, 0.1 mg ml^{-1} BSA (20). The activities of purified rFas2 and of the Fas2 mutants were monitored by inhibition of 5–10 pM AChE after a 1-h incubation at 37 °C and 14–18 h at room temperature.

Characterization of the Mutants—Culture media, 72 h after transfection, were screened for immunoreactivity and inhibitory activity directly or after 10–20-fold concentration by ultrafiltration. The Fas2 mutants were titrated by RIA, and their inhibitory activities were quantitated by AChE inhibition assay after partial purification and concentration by cation exchange of the media (100–200 ml) and ultrafiltration of the chromatographic fractions. The Fas2 mutants were submitted to at least two independent transfection-chromatography-assay sequences.
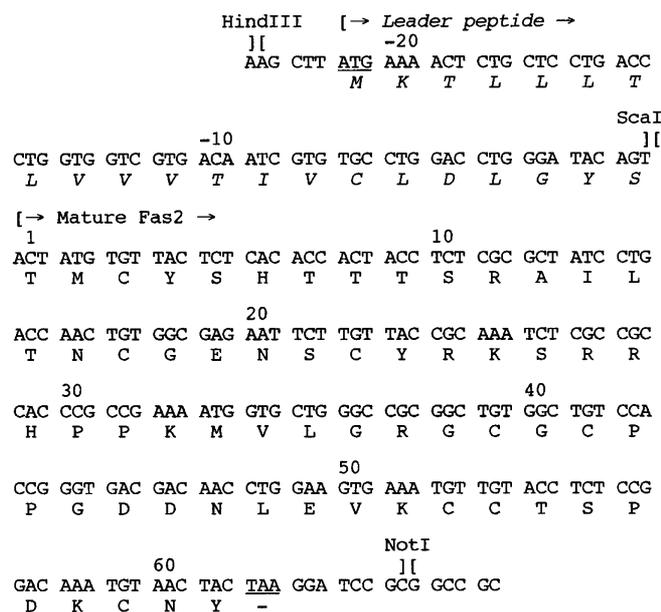
```
HindIII     [→ Leader peptide →
      ][                  -20
      AAG CTT ATG AAA ACT CTG CTC CTG ACC
              M   K   T   L   L   L   T

                                        ScaI
        -10                            ][
CTG GTG GTC GTG ACA ATC GTG TGC CTG GAC CTG GGA TAC AGT
L   V   V   V   T   I   V   C   L   D   L   G   Y   S

[→ Mature Fas2 →
1                               10
ACT ATG TGT TAC TCT CAC ACC ACT ACC TCT CGC GCT ATC CTG
T   M   C   Y   S   H   T   T   T   S   R   A   I   L

                20
ACC AAC TGT GGC GAG AAT TCT TGT TAC CGC AAA TCT CGC CGC
T   N   C   G   E   N   S   C   Y   R   K   S   R   R

     30                              40
CAC CCG CCG AAA ATG GTG CTG GGC CGC GGC TGT GGC TGT CCA
H   P   P   K   M   V   L   G   R   G   C   G   C   P

                    50
CCG GGT GAC GAC AAC CTG GAA GTG AAA TGT TGT ACC TCT CCG
P   G   D   D   N   L   E   V   K   C   C   T   S   P

                          NotI
          60            ][
GAC AAA TGT AAC TAC TAA GGA TCC GCG GCC GC
D   K   C   N   Y   -
```

FIG. 1. **Nucleotide and amino acid sequences of the chemically synthesized cDNA encoding rFas2.** The nucleotide sequence was designed from frequent mammalian codon usage and flanked on the 5' end by the sequence encoding the signal peptide of erabutoxin a (36). Positive numbering of the encoding amino acid sequence starts at the first residue of the processed rFas2. Initiation and termination codons are *underlined*, and relevant restriction sites are indicated.

RESULTS

Recombinant Wild-type Fasciculin

Expression of rFas2 in CHO Cells and Purification—Synthesis of the oligonucleotides encoding rFas2 enabled us to use codons of high usage frequency for mammalian cells and place restriction sites at convenient locations within the open reading frame and flanking regions. To ensure secretion and processing, a sequence encoding the leader peptide of a structurally related three-fingered toxin, erabutoxin a (36), was joined at the 5' end (Fig. 1). A *ScaI* site was generated at the linkage between the two sequences by replacing Thr at position -1 by Ser.

Selected clonal cells at confluence secreted up to 1.7 μg ml^{-1} (0.25 μM) of rFas2 in the 3-day intervals between medium changes; this rate continued for up to 10 weeks. Purification employed three steps on 500-ml batches of media (Fig. 2). Initial cation exchange led to removal of most medium proteins with a 440-fold enrichment (in pmol of Fas2 per mg of total protein) in rFas2, with more than 90% of recovery (Fig. 2A). A gel-filtration step purified rFas2 1500-fold (Fig. 2B). Final removal of trace contaminants was achieved by a second cation-exchange chromatography performed in isocratic conditions (Fig. 2C). rFas2 migrated in the same positions as the venom-derived Fas2 in the second and third chromatographic steps. An overall purification of 2200-fold was achieved in $\sim$50% yield.

Physical and Biological Characterization of rFas2—SDS-PAGE in reducing conditions (Fig. 3, *inset*) and isoelectric focusing analysis (not shown) each revealed a single, sharp band that migrated at a position identical to the venom-purified Fas2. Parallel runs on the amino acid analyzer yielded identical compositions for rFas2 and Fas2. Amino-terminal sequencing of native rFas2 yielded a single sequence, TMXY-SHTTTS, identical to that of Fas2, with a blank third step (noted as X) for non-reduced Cys^3. UV absorbance of natural Fas2 was used to estimate concentration of rFas2 stocks. Radioimmuno- and AChE-inhibition assays showed equivalent
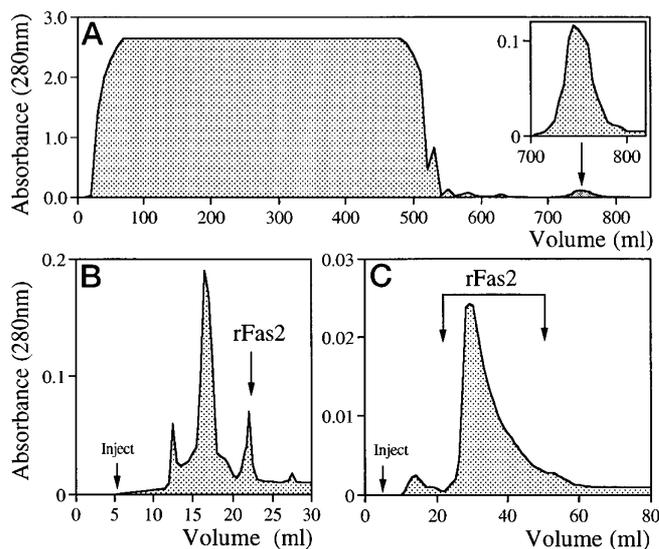

FIG. 2. **Three-step purification of rFas2 by FPLC.** *A*, rFas2 was concentrated and partially purified from the cell culture medium using cation exchange and elution with a NH$_4$Ac concentration gradient. Note the amounts of proteins (including rFas2) that are retained *versus* not retained by the column; *inset*, magnification of the rFas2 elution peak. *B*, the rFas2 fraction was further purified by gel filtration; rFas2 elutes in the included peak. *C*, final purification of rFas2 from trace contaminants was achieved by cation exchange under isocratic conditions, which accounts for the skewed peak.
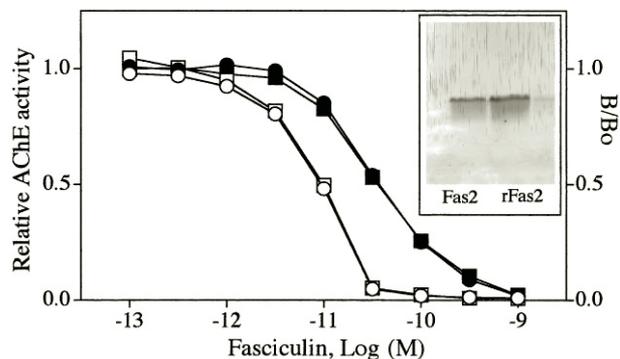
FIG. 3. **Biological and physical characterization of purified rFas2, compared to the venom-derived Fas2.** The concentrations of the Fas2 and rFas2 stock solutions were calculated from their UV spectra ($\epsilon_{276 \text{ nm}}$ = 4900 M^{-1} cm^{-1}). In this inhibition assay, Fas2 (○) and rFas2 (□) were incubated with $\sim$20 pM mouse AChE; a similar superimposition of the Fas2 and rFas2 curves was also observed when 5 pM AChE was used. In this RIA, Fas2 (●) and rFas2 (■) were incubated with ^{125}I-Fas2 (10,000 cpm) and a 100,000-fold dilution of the anti-Fas2 serum; B and B_o denote amounts of ^{125}I-Fas2 specifically bound by the anti-Fas2 serum in the presence and in the absence of competing ligand, respectively. Data points correspond to the average value of quadruplicates that differed by less than 5%. *Inset*, SDS-PAGE of rFas2 and Fas2 under denaturing conditions.

potencies for rFas2 and venom-derived Fas2 for inhibiting mouse AChE and competing with ^{125}I-Fas2 for binding to a polyclonal anti-Fas2 serum (Fig. 3 and Table I). Hence fully processed and correctly folded rFas2 is directly produced in mammalian cells.

Mutant Fasciculins

Selection of Positions for Mutation of Fas2—The overall net positive charge ($+4$ at neutral pH) of Fas2, coupled with its association at a peripheral anionic site on AChE, suggested an electrostatic attractive component with the cationic amino acids on Fas2 (Fig. 4). Cationic positions unique to the fasciculins were considered first. Hence, Arg^{11}, Arg^{24}, Lys^{25}, Arg^{27}, Arg^{28}, Lys^{32}, and Lys^{51} were mutated, but Arg^{37} and Lys^{58}, being

TABLE I

Relative inhibitory activities and apparent dissociation constants (K_i') of the recombinant wild-type and mutant fasciculins for mouse AChE

The relative inhibitory activity of the purified rFas2 was determined in the presence of 5 pM AChE (*cf.* legend to Fig. 3). The relative inhibitory activities of the transiently expressed rFas2 and mutants, monitored with 5 or 10 pM AChE, were calculated from ratios of dilutions for 50% inhibition and competition in the inhibition and radioimmunoassay titrations, respectively (*cf.* Fig. 6); the values were normalized to ratios with the venom-derived Fas2. Apparent K_i' values are expressed relative to the K_i value of Fas2 for mouse AChE (2.3 pM) (21). Data are from the major peak when more than a single peak appeared on the cation-exchange resin (*cf.* Fig. 5); *n*, number of independent experiments.

Fasciculin	Relative inhibitory activity[a] (normalized to Fas2)	Apparent K_i'
		pM
Wild-type		
rFas2 (purified)	1.00 ± 0.05 (*n* = 4)	2.3 ± 0.1
rFas2 (transient)	0.98 ± 0.26 (*n* = 5)	2.3 ± 0.6
Loop I mutations		
T8A/T9A	18 ± 13 (*n* = 3)	≤2.3
R11Q	6.3 ± 3.1 (*n* = 2)	≤2.3
Loop II mutations		
R24T	0.080 ± 0.003 (*n* = 2)	29 ± 1
K25L	1.08 ± 0.06 (*n* = 5)	2.1 ± 0.1
R27W	0.021 ± 0.017 (*n* = 3)	112 ± 91
R28D	1.10 ± 0.05 (*n* = 3)	2.1 ± 0.9
H29D	73 ± 21 (*n* = 3)	≤2.3
ΔP30	0.0052 ± 0.0065 (*n* = 4)	440 ± 550
P31R	0.0016 ± 0.0002 (*n* = 2)	1440 ± 180
K32G	0.32 ± 0.12 (*n* = 3)	7.2 ± 2.7
M33A	0.13 ± 0.05 (*n* = 2)	17.7 ± 6.8
V34A/L35A	0.93 ± 0.60 (*n* = 2)	2.5 ± 1.6
Loop III mutations		
D45K	0.7 ± 0.1 (*n* = 3)	3.3 ± 0.5
K51S	1.08 ± 0.01 (*n* = 2)	2.1 ± 0.02

[a] Values are shown as average ± the variation (*n* = 2) and means ± S.D. (*n* > 2).

invariant among the three-fingered toxins and with their side-chains only partly solvent-accessible (41, 42), were not studied. Second, His[29], supposedly unprotonated at neutral pH, is located at the tip of loop II, a position corresponding to the critical Asp[31] in erabutoxin a (43). Third, Pro[31], whose *cis* configuration constrains the conformation of the tip of loop II (30, 41), was modified to Arg, a residue and position essential for the α-neurotoxin activity (43, 44). Fourth, a doublet of anionic residues, Asp[45]-Asp[46], at the tip of loop III, is found only in the fasciculins and "synergistic-type" toxins, all from mamba venoms (45). All α-neurotoxins have a positively charged residue at position 45. Finally, the recently solved structures of two Fas2-AChE complexes (30, 31) revealed that several neutral residues participate in the interaction of Fas2 to AChE. Hence, Thr[8]-Thr[9], Pro[30], Met[33], and Val[34]-Leu[35], were also mutated.
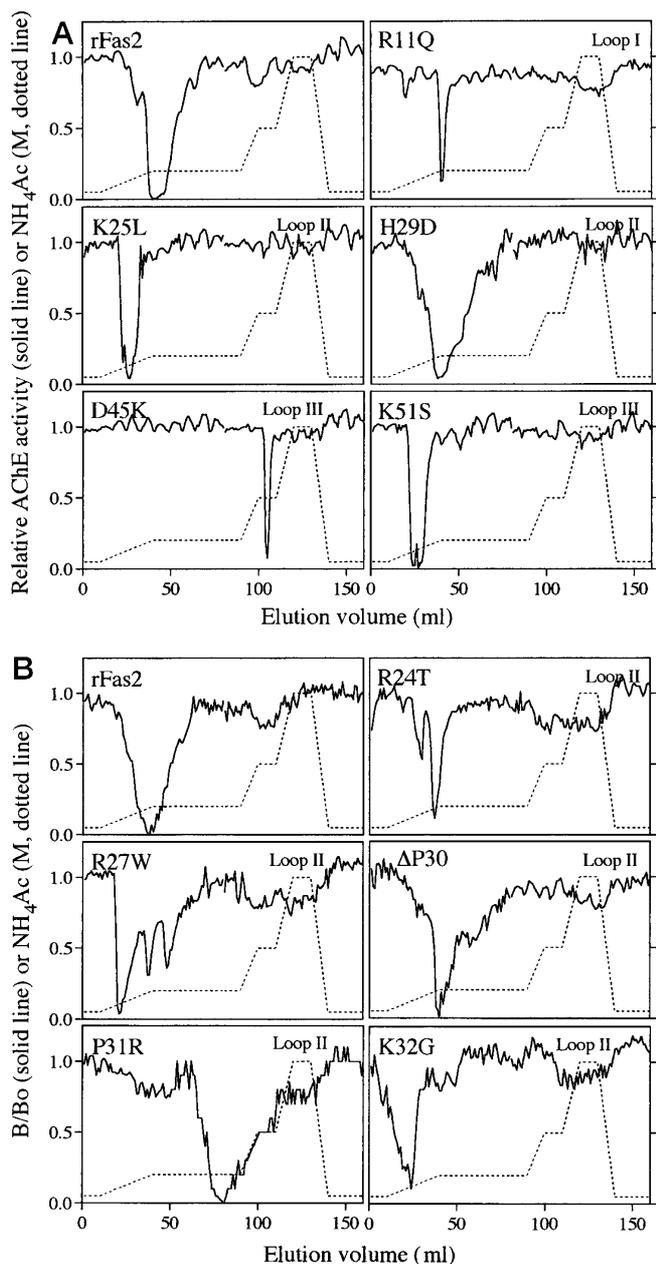
By substituting residues found in homologous toxins, perturbations in secondary structure might be minimized. Based on sequence homology and superimposition of crystal structures in the members of the three-fingered peptide family, Fas2, erabutoxin b, α-cobratoxin, α-bungarotoxin, and cardiotoxin VII4 (Fig. 4*A*), we mutated Arg[11] → Gln (R11Q), Arg[24] → Thr (R24T), Lys[25] → Leu (K25L), Arg[27] → Trp (R27W), Arg[28] → Asp (R28D), His[29] → Asp (H29D), Pro[31] → Arg (P31R), Lys[32] → Gly (K32G), Asp[45] → Lys (D45K), and Lys[51] → Ser (K51S) (Fig. 4*B*). The close fit and potential for hydrogen bonding of certain residues at the binding interface of the Fas2-AChE complex suggested that side chains on Thr[8], Thr[9], Met[33], Val[34], and Leu[35] be minimally perturbed. Accordingly, we changed them into Ala (T8A/T9A, M33A, and V34A/L35A mutants). Finally, to shorten loop II and possibly create a gap between the bound Fas2 and the entrance of the gorge of the enzyme, we deleted Pro[30] (ΔP30 mutant).

Transient Expression of Fas2 Mutants in HEK Cells—Expression from transiently transfected cells enabled direct analysis of activity and/or peptide production in the cell culture media. Analysis of AChE inhibition and RIA titer allowed an initial classification of the Fas2 mutants. Class I comprised the T8A/T9A, K25L, R28D, H29D, D45K, V34A/L35A, and K51S mutants, which displayed significant AChE inhibition and immunoreactivity. Class II comprised the R24T, R27W, ΔP30, P31R, K32G, and M33A mutants, which displayed significant immunoreactivity but less AChE inhibition. Class III comprised only the R11Q mutant, which displayed AChE inhibition but in complete curves immunoreactivity curves. Production yields, determined by RIA titration of rFas2 and the Fas2 mutants secreted into the media, ranged between 0.5 and 5 pmol ml^{-1} in a 3-day period.

Chromatography of the Fas2 Mutants—Elution positions of the Fas2 mutants on the cation-exchange resin were monitored by RIA and AChE inhibition assay for the class I and class III mutants and by RIA for the class II mutants. Representative profiles are shown in Fig. 5. Compared to rFas2 (*top panels*), 10 of the 14 mutants showed elution positions consistent with their net charge. Mutants T8A/T9A, ΔP30, M33A, and V34A/L35A, all possessing the same net charge as rFas2, eluted at the same ionic strength as rFas2. Mutants K25L, R27W, K32G, and K51S, which lost one net positive charge, eluted at lower ionic strength than rFas2. Mutants P31R and D45K, which gained one and two net positive charge(s), eluted at higher ionic strengths than rFas2. In contrast, mutants R11Q, R24T, R28D, and H29D, which lost either one or two positive charge(s), eluted at a similar ionic strength as rFas2, suggesting that the initial and newly introduced side chains at positions 11, 24, 28, and 29 are not solvent-accessible and/or do not interact with the anionic matrix of the column. Two mutants, R24T and R27W, eluted as several peaks, but calculation of concentrations based on a simple reversible equilibrium for ligand binding revealed that the additional peaks are minor components. Whether these peaks reflect incomplete processing or folding of the peptides, or slow conformational equilibria, has not been ascertained.

Analysis of the Apparent Dissociation Constants (K_i') of the Fas2 Mutants—The Fas2 mutants, enriched in purity and concentrated by cationic exchange and ultrafiltration, were titrated by RIA and analyzed for inhibitory activity (Fig. 6). The RIA profiles were generally consistent with the amounts of peptide expected based on transfection efficiency and purification yields. In contrast, the concentration dependences of the AChE inhibition curves, relative to those of immunoreactivity, varied widely, illustrating significant differences in the affinities of the Fas2 mutants for AChE. The transiently expressed rFas2 sample, enriched and concentrated, yielded the same AChE inhibition potency as the stably expressed and fully purified rFas2 (*cf.* Fig. 3). Compared to rFas2, no significant differences in inhibition potency were found for mutants K25L, R28D, K32G, V34A/L35A, D45K, and K51S. In contrast, significant differences were found for mutants T8A/T9A, R11Q, R24T, R27W, H29D, ΔP30, P31R, and M33A. The inhibitory activities of the Fas2 mutants toward mouse AChE, calculated from the dilutions for 50% inhibition in the inhibition assays and 50% competition in the RIA titrations, and normalized to Fas2, are reported in Table I. The apparent K_i' values that are also reported are expressed relative to a K_i value of 2.3 pM for Fas2 (21). Because of the limitations that may arise from slow equilibration, from the disparity between added and free ligand, and from using immunoreactivity to reflect peptide concentration, the mutants with low dissociation constants are specified only by an upper limit.

A

```
                  1        10        20         30        40        50        60
                  |        |         |          |         |         |         |
      Fas2        TMCYSHTTTSRAILTNC-G-E-N-SCYRKSR-RH---PP-KMVLGRGC--G--CPPGDDNLEVKCCTSPDKCNY
                  |        |         |          |         |         |  || |
      Erabutx     RICFNHQSSQPQTTKTC-SPG-ESSCYHKQW-SD---FR-GTIIERGC--G--CPTVKPGIKLSCCESEV-CNN
                  |        |         |          |         |         |  || |
      α-Cobratx   IRCFITP-DIT--SKDC-P-NGH-VCYTKTWCDAFCSIR-GKRVDLGCAAT--CPTVKTGVDIQCCS-TDNCNPFPTRKRP
                  |        |         |          |         |         |  || |
      α-Bungtx    IVCHTTATIPSSAVT-CPP-G-ENLCYRKMWCDAFCS-SRGKVVELGCAAT--CPSKKPYEEVTCCS-TDKCNHPPKRQPG
                  |        |         |          |         |         |  || |
      Cardiotx    LKCNK-LIPI-A-YKTCPE-G-KNLCYKMML-AS---KK-MVPVKRGC--INVCPKNSALVKYVCCS-TDRCN
                  |---Loop I----|       |-------Loop II-------|    |-Loop III-|
```

B

```
                  1        10        20         30        40        50        60
                  |        |         |          |         |         |         |
      Fas2        TMCYSHTTTSRAILTNCGENSCYRKSRRHPPKMVLGRGCGCPPGDDNLEVKCCTSPDKCNY  (+4)
      Fas2 mutants:
      T8A-T9A     .......AA....................................................  (+4)
      R11Q        ..........Q.................................................  (+3)
      R24T        ...............................T............................  (+3)
      K25L        ................................L...........................  (+3)
      R27W        ..................................W.........................  (+3)
      R28D        ...................................D........................  (+2)
      H29D        ....................................D.......................  (+3)
      ΔP30        .....................................(  )...................  (+4)
      P31R        ......................................R.....................  (+5)
      K32G        .......................................G....................  (+3)
      M33A        ........................................A...................  (+4)
      V34A-L35A   .........................................AA................  (+4)
      D45K        ...................................................K........  (+6)
      K51S        .........................................................S...  (+3)
                  |----LoopI----|      |-----LoopII-----| |--LoopIII-|
```

FIG. 4. **Sequence alignments.** *A*, alignment of three-fingered toxins of known three-dimensional structure was generated with HOMOLOGY (Biosym Technologies, Inc., 1994) by optimization of the superimposition of the crystal structures of Fas2 (entry code, 1FSC), erabutoxin b (3EBX), α-cobratoxin (1CTX), α-bungarotoxin (2ABX), and cardiotoxin V^{II}_4 (1CDT) according to their backbone atoms. The amino acid numbering corresponds to Fas2 numbering. The *bars* between the sequences indicate the conserved disulfide bridges; note the extra bridge within loop II of the two long neurotoxins. The residues *underlined* in the Fas2 sequence have been mutated. The residues *underlined* in the other toxin sequences correspond to some of the studied substitutions (see text). *B*, amino acid sequences of the wild-type and mutant fasciculins. For clarity, only the substitutions made on the Fas2 sequence are displayed. The values on the *right* indicate the theoretical net charge of the proteins at neutral pH, with the His residues assumed to be unprotonated.

Residue Contributions to Fas2 Inhibition Based on Mutagenesis Studies—Based on the relative inhibitory activities of the rFas2 mutants (Table I), the mutations can be classified in four categories: (i) those which cause little or no apparent effect on Fas2 activity, as seen for mutants K25L, R28D, V34A/L35A, D45K, K51S (no change), or K32G (3-fold decrease), (ii) those which cause a decrease by about one order of magnitude in the Fas2 activity, as seen for mutants R24T (13-fold) and M33A (8-fold), (iii) those which cause a decrease by two or more orders of magnitude, as seen for mutants R27W (49-fold), ΔP30 (192-fold), and P31R (625-fold), and (iv) those which cause an apparent increase in the Fas2 inhibitory activity, as seen for mutants T8A/T9A, R11Q, and H29D (18-, 6-, and 73-fold, respectively).

The contribution of the mutated residues to activity, relative to their location in the three-dimensional structure of Fas2 bound to mouse AChE (30), is shown in Fig. 7. The three residues that dominate the AChE-inhibitory activity of Fas2, Arg[27], Pro[30], and Pro[31], form a subset located at the tip of loop II. The surface area of this subset, 261 Å^2, represents only 6% of the total accessible surface area of Fas2 but 25% of the Fas2 area buried in the Fas2-mAChE complex. Fas2 residues Thr[8], Thr[9], and Arg[11], mutation of which resulted in an apparent increase in Fas2 activity, form a second subset located at the tip of loop I. The surface area of this subset, 300 Å^2, represents 7% of the total accessible surface area of Fas2 but 29% of the Fas2 area buried in the complex. Hence, a small fraction of the many Fas2 residues which make up the overall functional site provide the critical contacts required for the high affinity interaction.

DISCUSSION

Several groups have produced recombinant three-fingered snake toxins, α- and κ-neurotoxins, as fusion proteins in heterologous bacterial expression systems, and some have reported site mutagenesis studies on these toxins (43, 44, 46–52). The lower activity of the fusion proteins, compared to the natural toxins, however, precludes direct analysis of the mutants before *in vitro* cleavage of the hybrid by chemical or enzymatic means. More recently, a recombinant κ-neurotoxin was produced in yeast with full activity, although possessing a short amino-terminal extension due to altered signal peptide cleavage (53). In our study, we used a mammalian system to express secreted and fully processed rFas2 and 14 Fas2 mutants. Direct expression of rFas2 in its functional conformation demonstrates that the use of the signal peptide sequence of erabutoxin a and the change at position −1 were not critical for post-translational events such as folding, cleavage of signal peptide, and disulfide bond formation of the rFas2 molecule in mammalian cells.

Owing to the use of complementary assays, RIA titration and AChE inhibition, 14 transiently expressed Fas2 mutants could be quantitated and functionally characterized without extensive purification. The polyclonal anti-Fas2 serum is characterized by a high titer in antibodies, likely to be mostly IgGs (35). The shapes of the RIA curves, that generally extend over a concentration range wider than expected for interaction of ^{125}I-Fas2 with a single site (Figs. 3 and 6), suggest that the serum contains at least two IgG populations presumably directed

FIG. 5. **Cation-exchange chromatography of rFas2 and rFas2 mutants.** *A,* the chromatographic fractions were monitored for Fas2 activity on mouse AChE for rFas2 (120 ml of culture medium were loaded, 5 μl of each fraction were assayed) and for mutants R11Q (110 ml, 50 μl), K25L (85 ml; 5 μl), H29D (200 ml; 15 μl), D45K (50 ml; 5 μl), and K51S (85 ml; 5 μl); mutants T8A/T9A (165 ml; 5 μl) and R28D (100 ml; 5 μl) are not shown. *B,* the fractions were monitored for reactivity toward a polyclonal anti-Fas2 serum for rFas2 (sample loaded, 150 ml) and for mutants R24T (175 ml), R27W (175 ml), ΔP30 (150 ml), P31R (160 ml), and K32G (200 ml); mutants M33A (185 ml) and V34A/L35A (165 ml) are not shown; 50 μl of each fraction were assayed in each case; *B* and B_o denote the amounts of ^{125}I-Fas2 specifically bound by the anti-Fas2 serum in the presence and the absence of competing ligand, respectively. The empty pGS vector (sample loaded, 145 ml) yielded no signal for both AChE inhibition (15 μl of each fraction were assayed) and RIA screenings (50 μl were assayed). The absorbance profiles (280 nm) arose primarily from absorption of the culture medium proteins (not shown).

toward distinct epitopes on Fas2. The existence of several antigenic determinants on the fasciculin molecule is in accord with previous reports of three to four distinct epitopes simultaneously accessible to specific antibodies (Fab fragments) directed against α-neurotoxins and of two monoclonal antibodies
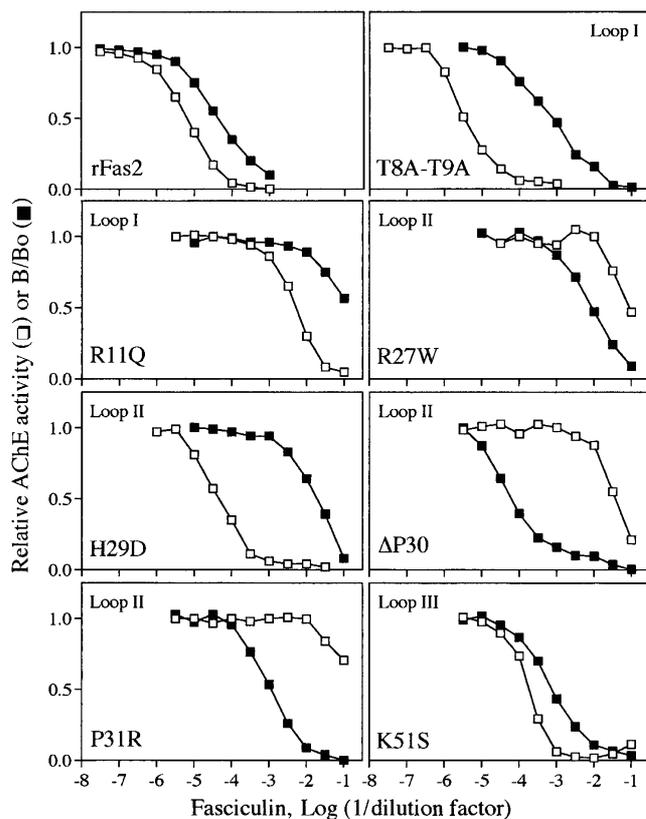
FIG. 6. **Comparative AChE inhibition and radioimmunoassays of rFas2 and Fas2 mutants (primary data).** The rFas2 and mutant rFas2 enriched fractions eluted from the cation-exchange column (*cf.* Fig. 5) were dialyzed and concentrated by ultrafiltration. The AChE inhibition assays ($\square$) were performed with 5 or 10 pM mouse AChE. The RIAs ($\blacksquare$) were performed with ^{125}I-Fas2 (10,000 cpm) and the anti-Fas2 serum at its titer; *B* and B_o denote amounts of ^{125}I-Fas2 specifically bound by the anti-Fas2 serum in the presence and in the absence of competing ligand, respectively. For rFas2, note that the relative positions of the AChE inhibition and RIA curves are similar to those obtained with purified rFas2 (*cf.* Fig. 3). For the mutants, compare the positions of the curves for AChE inhibition relative to the RIA curves with those of rFas2 (*top panel*). For each curve, the dilution yielding 50% competition or inhibition was quantified by reference to an internal standard curve made with Fas2 (not shown). Data are from the major peak when the mutant yielded several peaks on the cation-exchange resin. Data points correspond to the average value of duplicates that differed by less than 5%. The relative Fas2 activities of the mutants, averaged from several experiments, are reported in Table I.

directed toward distinct areas of a cardiotoxin (*cf.* Ref. 54). Because of the heterogeneity of polyclonal antisera, as well as the multiplicity of residues involved in the contact area between each IgG and its specific epitope, single residue modifications of the three-fingered toxins usually have little influence on polyclonal antibody titers. Antigenic diversity proved to be generally useful for quantifying the loss in the inhibitory activity of the Fas2 mutants based on immunotitration of enriched samples.

Mutants T8A/T9A, R11Q, and H29D, however, displayed greater ratios of inhibitory activity to immunochemical titer than did wild-type Fas2. While this may reflect enhanced inhibitory affinity for AChE, several caveats preclude a precise determination of a dissociation constant. First, with a fasciculin dissociation rate constant of 4.0×10^{-3} min^{-1} (21), extended equilibration times are required for fractional AChE occupation. Extensive dilution of AChE to satisfy the condition of a K_i to total enzyme concentration ratio that assures a reasonable fraction of free ligand (55, 56) would have required unrealistic equilibration times for the putative high affinity
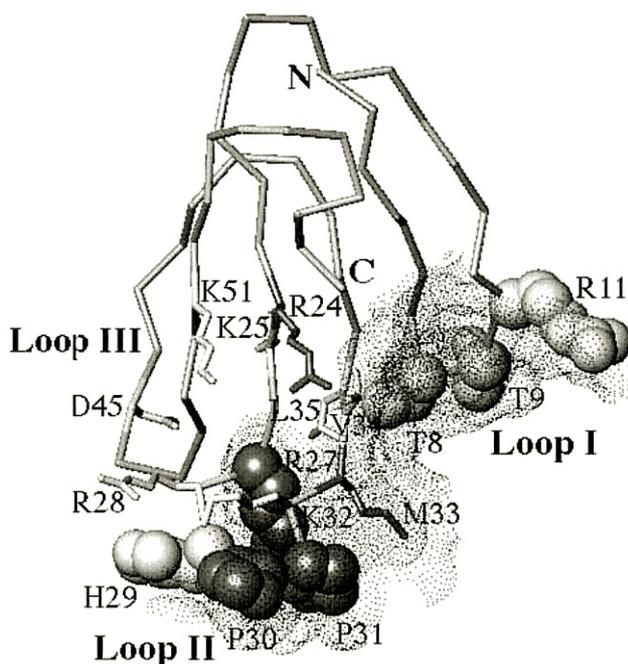
FIG. 7. **Positions of the functionally important residues of Fas2.** The three-dimensional structure of Fas2 complexed with mouse AChE (30) is viewed looking toward the concave side of the molecule; the molecular surface of mAChE buried in the complex is displayed (*dots*). The side chains of the Fas2 residues whose mutation causes virtually no effect on Fas2 activity are displayed as *light gray sticks* (K25L, R28D, K32G, V34A/L35A, D45K, and K51S). Those whose mutation causes a decrease by about one order of magnitude in Fas2 activity are displayed as *dark gray sticks* (R24T and M33A). Those whose mutation causes a decrease by two or more orders of magnitude in Fas2 activity are displayed as *dark gray* CPK (R27W, ΔP30, and P31R). Those whose mutation causes an apparent increase in Fas2 activity are displayed as *light gray* CPK (T8A/T9A, R11Q, and H29D). The two subsets of functionally important residues (CPK mode) reside at the tips of loop I and loop II, respectively. *N* and *C* denote the amino and carboxyl termini of the Fas2 molecule, respectively. This figure was generated with program TURBO-FRODO (70).

mutants. Second, as detailed below, the ratios will be artificially high if a region of Fas2 is a dominant epitope, as mutants of this region would show diminished immunoreactivity.

Mutations in Loop II—Loop II of Fas2 contains 16 residues, located between Cys[22] and Cys[39] (Fig. 4). Eleven residues, Arg[24], Lys[25], and all residues from Arg[27] through Leu[35], were mutated. The Arg[27]-Pro[30]-Pro[31] subset dominates the inhibitory activity of Fas2 (Figs. 6 and 7 and Table I) and interacts with the peripheral anionic site of the enzyme (30). However, the influence of these mutations is particularly complex since they may cause at least three distinct changes. Substitution of Trp for Arg[27] removes a positive charge, increases the volume of the side chain, and introduces an aromatic indole ring with hydrophobic properties. Thus, the specific conformation of Fas2 loop II is likely to be altered because of the loss of the stabilizing intraloop interaction that Arg[27] establishes with Pro[30] and its indirect influence on the Pro[30]-*cis*-Pro[31] turn (30, 41). The bulky Trp side chain introduced at position 27 should experience steric hindrance with mAChE-Trp[286] and would eliminate the potential hydrogen bonds of Arg[27] with the carbonyl oxygens of Trp[286] and Leu[289] in mAChE. A similar steric occlusion might be responsible for the increased K_i seen for Fas2 chemically modified at Arg[27] (57). Deletion of the amino acid residue Pro[30] not only removes the cyclic side chain, but also alters both the length of loop II and the *cis* conformation of its tip. As a result, the cavity formed by mAChE residues Glu[292], Ser[293], Gly[342], and Ile[365] is likely to contain bound water molecules in

the complex. The shrinking of loop II, as well as its enhanced flexibility, would diminish the high complementarity of the interactive surface seen in the crystal structure (30). Substitution of Arg for Pro[31] increases side chain dimensions, introduces a positive charge, and perhaps precludes formation of the *cis* bond in Pro[30]. The obvious consequences would be steric hindrance of the bulkier Arg side chain with the cluster formed by mAChE residues Leu[289], Ser[293], and Tyr[341], as well as Coulombic repulsion with Fas2-Lys[32] and/or mAChE-Arg[296] (30). To resolve these possible interactions, residue substitutions at positions 27, 30, and 31 with progressive changes in side chain properties may help delineate the respective contributions of the charge, volume, and stereochemical characteristics of these three residues to conformation and stability of the complex.

Both the substitutions of Thr for Arg[24] and Ala for Met[33] resulted in an order of magnitude decrease in Fas2 activity (Table I). Arg[24], located at the base of loop II (Fig. 7), is a structurally important residue that stabilizes the carboxyl-terminal and core regions of Fas2 through hydrogen bonding to the carbonyl atom of Tyr[61] and stacking interaction with Arg[37] (30, 41). None of these interactions should be retained by the shorter, uncharged Thr side chain. Thus, a less stable complex forms with mAChE because of indirect destabilization of the mutated peptide molecule. The Met[33] → Ala mutation should have a more direct influence. The loss of the sulfur atom and shortening of the side chain preclude stacking interactions with Trp[286] and van der Waals contacts with Tyr[341], two key mAChE residues located at the peripheral anionic site (21, 58, 59). In addition, the smaller Ala side chain cannot retain secondary hydrophobic interactions with mAChE residues Tyr[72], Tyr[124], and Tyr[341] (30). In the Fas2-mAChE complex, most of the solvent-accessible surface area of Met[33] is lost; in fact, this residue contributes about 10% of the Fas2 surface area buried at the interface (30), a value slightly greater than the individual contributions of neighboring critical Fas2 residues Arg[27], Pro[30], and Pro[31]. On the other hand, of the several peripheral anionic site residues that interact with Met[33], a single one, Tyr[124], does not establish any other contact with Fas2 (30). A decrease in apparent affinity for Fas2 of two orders of magnitude was observed for mAChE mutant Y124Q (21). More than a single order of magnitude in the decrease in Fas2 activity could therefore have been expected upon mutation of Met[33]; however, the minimal change in the side chain volume with an Ala substitution likely preserves the tight fit of the other loop II residues with the peripheral anionic site.

Substitutions of Leu for Lys[25], of Asp for Arg[28], and of an Ala doublet for Val[34]-Leu[35], resulted in unaltered Fas2 activity (Table I). These results are in accord with the crystallographic observations that show that the Lys[25] and Arg[28] side chains point away from the Fas2-mAChE interface, and that cavities exist between the van der Waals surfaces defined by the side chains of Fas2 residues Val[34] and Leu[35] and mAChE residues Leu[76], Tyr[72], and His[287], respectively (30). Replacement of Arg[28] by Asp probably induces structural rearrangements leading to a different network of internal charge compensation; surprisingly, this does not perturb the activity of the mutant toward the enzyme.

Substitution of Asp for His[29] resulted in an apparent increase of two orders of magnitude in the Fas2 activity (Figs. 6 and 7 and Table I). In the crystalline complex, the side chain of His[29] participates in van der Waals interactions with mAChE-Glu[292] that the newly introduced Asp side chain, negatively charged, cannot establish because of charge repulsion (30). However, the Asp side chain may be sufficiently flexible to rotate toward the side chain of either Arg[27] or Arg[28] and

undergo charge compensation. Also, an internal salt bridge could form with Arg[27]. Thus, an improved fit of the more rigid tip of loop II with the mAChE peripheral anionic site residues might result from stabilization of internal structure. However, as discussed below, a change in structure might also affect the immunoreactivity of this mutant.

Mutations in Loop I—Loop I of Fas2 encompasses 13 residues, located between Cys[3] and Cys[17] (Fig. 4). Both the mutations made on Thr[8]-Thr[9] and Arg[11] lead to apparent increases of one order of magnitude in the activities of the mutants toward mAChE (Fig. 6 and Table I). The Thr[8]-Thr[9]-Arg[11] subset is fully exposed at the tip and external edge of loop I (Fig. 7), which fits in a crevice near the lip of the mAChE catalytic gorge and maximizes the surface area of contact of loop II at the gorge entry (30). In particular, the Thr[8]-Thr[9] doublet potentially interacts with eight mAChE residues, Tyr[70], Gln[71], Tyr[72], Val[73], Leu[92], Gln[279], Val[282], and Asp[283] (30). Substitution of an Ala doublet eliminates hydrogen bonding of the Thr side chains with Gln[279] and Asp[283]. The smaller size of the two Ala side chains might facilitate a rearrangement of the backbone at the tip of loop I, enabling it to come closer to loop II and establish a stabilizing internal interaction with Fas2-Leu[35]. In addition, the smaller side chain of Ala[9] may establish more favorable interactions with mAChE residues Tyr[70], Leu[92], and Val[282] and provide a tighter fit of the tip of loop I with the furrow that exists on the mAChE surface (30), possibly compensating for the loss of hydrogen bonding energy. On the other hand, Arg[11] hydrogen bonds with mAChE-residues Glu[84] and Asn[87]. Substitution of Gln for Arg[11] likely preserves the capacity for hydrogen bonding, especially as the smaller size of the Gln side chain should favor a tighter fit between the tip of loop I and the enzyme. Internal stabilization of the Fas2 molecule and/or loop I anchorage at the enzyme surface could thus contribute to tighter occlusion, by the tip of loop II, of the catalytic site gorge of the enzyme. Incidentally, the apparent increase in Fas2 activity that results from the removal of the positive charge does not match with the 40–73% loss in the activity of Fas2 chemically modified at Arg[11] (57). The modifying agent, however, produces a substantial enlargement in the effective side chain that is not reproduced by the Gln mutation.

Although infrequent, single residue substitutions have shown enhanced affinity with the three-fingered peptidic toxins. The 35-fold higher affinity of Fas3, compared to Fas1, for rat brain AChE likely results from the Thr[15] → Lys substitution in loop I (20). Substitution of Arg for Ile[36] in erabutoxin a loop II led to a 7-fold increase in this neurotoxin's affinity for the nicotinic receptor (44). Two mutations of *Bungarus* AChE, near the presumed peripheral site, resulted in up to a 14-fold increase in affinity for Fas2 (22). Nevertheless, the uncertainties in the relative activities of the Fas2 mutants T8A/T9A, R11Q, and H29D preclude accurate determinations of specific activity without the availability of homogeneous peptides.

In several three-fingered toxins, the edge of the first loop and the tip and concave side of the second loop are domains immunoreactive to monoclonal antibodies. In Fas2, the bulky side chains of Arg[11] and His[29] could be particularly immunogenic, as was found for Trp[11] of a cardiotoxin, toxin γ, and Lys[15] of a neurotoxin, toxin α (54). Thus, apart from the structural arguments that may explain increased inhibitory activity, the Arg[11] → Gln and His[29] → Asp mutations may also have altered dominant epitopes located on loop I and loop II. Hence, a diminished, although not eliminated, recognition of the mutant by the anti-Fas2 serum (Fig. 6) may result in an overestimation of their relative inhibitory activities toward AChE. Similar considerations could influence our results for the double mutant T8A/T9A.

Despite the unique conservation of Arg[11] in the fasciculins (42), the cationic side chain at this position does not appear to be a major contributor to the affinity nor to the inhibitory capacity of Fas2. In the crystalline complex, Arg[11] associates with the region of Trp[86], proposed as a second portal, or "back door," for substrate entry into the enzyme (60, 61). Should translation of the choline cation through the putative back door region be rate-limiting in catalysis in the Fas2-AChE complex, a greater influence of Arg[11] on AChE inhibition by Fas2 would have been expected. The side chain of Arg[11], however, displays high temperature factors (B factors) not only in the structures of unbound Fas1 and Fas2 (41, 62), but also in those of Fas2 bound to mAChE and *Torpedo* AChE (30, 31). In general, the highly flexible loop I may adopt an ensemble of conformations (41, 62); yet, a single conformation is selected in the formation of the high affinity complex (30, 31).

Mutations in Loop III—Loop III of Fas2 encompasses 10 residues, located between Cys[41] and Cys[52] (Fig. 4). The unaltered Fas2 activities of the D45K and K51S mutants (Figs. 6 and 7 and Table I) are consistent with the lack of interaction of residues Asp[45] and Lys[51] with mAChE, as observed in the crystalline complex. Yet, in the fasciculins, compared to the other members of the three-fingered toxin family, the Asp[45]-Asp[46] doublet confers to loop III an exclusive anionic locus which dictates the orientation of the dipole vector of the molecule (18, 42). An internal structural rearrangement in the D45K mutant molecule may occur, since the Lys side chain introduced at position 45 should repel Arg[28], which stabilizes Asp[45] in Fas2 (41, 42). In the mutant, however, it may be compensated by the neighboring side chain of Asp[46].

Changes in the Fas2 structure have been proposed earlier to explain the 57% decrease in Fas2 activity upon acetylation of Lys[51] (63). Two residues of loop III, Asn[47] and Leu[48], interact with mAChE-His[287], but at distances of ~4 Å (30); however, Leu48 does not interact with *Torpedo* AChE (31). Loop III residues, therefore, likely play no critical functional role other than internal stabilization of loop II conformation.

Numerous aromatic residues reside at the Fas2-mAChE complex interface: Fas2-Tyr[4], His[6], His[29], and Tyr[61], and mAChE-Tyr[70], Tyr[72], Tyr[77], Tyr[124], Trp[286], His[287], Tyr[341], as well as several nonaromatic residues which undergo hydrophobic interactions: Fas2-Pro[30], Pro[31], and Met[33], and mAChE-Pro[78] (30). Mutation of Fas2-Pro[30] and Pro[31], which are central to the interface, resulted in two to three orders of magnitude decreases in Fas2 activity. Single-site substitutions of mouse AChE peripheral anionic site residues Tyr[72], Tyr[124], and Trp[286], also central to the interface, reduced the affinity of Fas2 by two to six orders of magnitude (21). Thus, patches of high hydrophobicity at the interface dominate the binding free energy of the Fas2-AChE complex, consistent not only with the tight intermolecular packing areas observed in the crystal structures (30, 31), but also with general structural patterns observed at interfaces of high affinity protein-protein complexes (64–69).

Site-directed mutagenesis of the Fas2 molecule and expression of the mutants from transiently transfected mammalian cells have provided substantial information on the respective contributions of 16 residues of Fas2 positioned for interaction with mouse AChE. The determinants identified by the structural and the functional approaches do coincide, but only a few of the many residues which make up the overall interactive site of the Fas2 molecule provide the strong interactions required for high affinity binding. Mutant cycle analyses, coupled with kinetic and crystallographic studies, should further delineate the contribution of individual residues to the affinity and inhibitory capacity of the fasciculin-AChE complexes.

REFERENCES

1. Lee, C. Y. & Chang, C. C. (1966) *Mem. Inst. Butantan (Sao Paolo)* **33,** 555–572
2. Changeux, J. P., Kasai, M. & Lee, C. Y. (1970) *Proc. Natl. Acad. Sci. U. S. A.* **67,** 1241–1247
3. Endo, T. & Tamiya, N. (1991) in *Snake Toxins* (Harvey, A. L., ed) pp. 165–222, Pergamon Press, New York
4. Chiappinelli, V. A. (1983) *Brain Res.* **277,** 9–22
5. Oswald, R. E., Sutcliffe, M. J., Bamberger, M., Loring, R. H., Braswell, E. & Dobson, C. M. (1991) *Biochemistry* **30,** 4901–4909
6. Adem, A., Asblom, A., Johansson, G., Mbugua, P. M. & Karlsson, E. (1988) *Biochim. Biophys. Acta* **968,** 340–345
7. Segalas, I., Roumestand, C., Zinn-Justin, S., Gilquin, B., Ménez, R., Ménez, A. & Toma, F. (1995) *Biochemistry* **34,** 1248–1260
8. de Weille, J. R., Schweitz, H., Maes, P., Tartar, A., & Lazdunski, M. (1991) *Proc. Natl. Acad. Sci. U. S. A.* **88,** 2437–2440
9. Albrand, J. P., Blackledge, M. J., Pascaud, F., Holleker, M. & Marion, D. (1995) *Biochemistry* **34,** 5923–5937
10. McDowell, R. S., Dennis, M. S., Louie, A., Shuster, M., Mulkerrin, M. G. & Lazarus, R. A. (1992) *Biochemistry* **31,** 4766–4772
11. Sutcliffe, M. J., Jaseja, M., Hyde, E. I., Lu, X. & Williams, J. A. (1994) *Struct. Biol.* **1,** 802–807
12. Bougis, P., Rochat, H., Piéroni, G. & Verger, R. (1981) *Biochemistry* **20,** 4915–4920
13. Dufton, M. J. & Hider, R. C. (1991) in *Snake Toxins* (Harvey, A. L., ed) pp. 259–302, Pergamon Press, New York
14. Drenth, J., Low, B. W., Richardson, J. S. & Wright, C. S. (1980) *J. Biol. Chem.* **255,** 2652–2655
15. Wright, C. S. (1987) *J. Mol. Biol.* **194,** 501–529
16. Kieffer, B., Driscoll, P. C., Campbell, I. D., Willis, A. C., van der Merwe, P. A. & Davis, S. J. (1994) *Biochemistry* **33,** 4471–4482
17. Ploug, M. & Ellis, V. (1994) *FEBS Lett.* **349,** 163–168
18. Karlsson, E., Mbugua, P. M. & Rodriguez-Ithurralde, D. (1984) *J. Physiol. (Paris)* **79,** 232–240
19. Cerveñansky, C., Dajas, F., Harvey, A. L. & Karlsson, E. (1991) in *Snake Toxins* (Harvey, A. L., ed) pp. 303–321, Pergamon Press, New York
20. Marchot, P., Khélif, A., Ji, Y.-H., Mansuelle, P. & Bougis, P. E. (1993) *J. Biol. Chem.* **268,** 12458–12467
21. Radic, Z., Duran, R., Vellom, D. C., Li, Y., Cervenansky, C. & Taylor, P. (1994) *J. Biol. Chem.* **269,** 11233–11239
22. Cousin, X., Bon, S., Duval, N., Massoulié, J. & Bon, C. (1996) *J. Biol. Chem.* **271,** 15099–15108
23. Radic, Z., Quinn, D. M., Vellom, D. C., Camp, S. & Taylor, P. (1995) *J. Biol. Chem.* **270,** 20391–20399
24. Eastman, J., Wilson, E. J., Cerveñansky, C. & Rosenberry, T. L. (1995) *J. Biol. Chem.* **270,** 19694–19701
25. Marchot, P., Ravelli, R. B. G., Raves, M. L., Bourne, Y., Vellom, D. C., Kanter, J., Camp, S., Sussman, J. L. & Taylor, P. (1996) *Protein Sci.* **5,** 672–679
26. Rosenberry, T. L., Rabl, C.-R. & Neumann, E. (1996) *Biochemistry* **35,** 685–690
27. Sussman, J. L., Harel, M., Frolow, F., Oefner, C., Goldman, A., Toker, L. & Silman, I. (1991) *Science* **253,** 872–879
28. Taylor, P. & Lappi, S. (1975) *Biochemistry* **14,** 1989–1997
29. Taylor, P. & Radić, Z. (1994) *Annu. Rev. Pharmacol. Toxicol.* **34,** 281–320
30. Bourne, Y., Taylor, P. & Marchot, P. (1995) *Cell* **83,** 503–512
31. Harel, M., Kleywegt, G. J., Ravelli, R. B. G., Silman, I. & Sussman, J. L. (1995) *Structure* **3,** 1355–1366
32. le Du, M. H., Marchot, P., Bougis, P. E. & Fontecilla-Camps, J. C. (1989) *J. Biol. Chem.* **264,** 21401–21402
33. Radić, Z., Pickering, N. A., Vellom, D. C., Camp, S. & Taylor, P. (1993) *Biochemistry* **32,** 12074–12084
34. Vellom, D. C., Radić, Z., Li, Y., Pickering, N. A., Camp, S. & Taylor, P. (1993) *Biochemistry* **32,** 12–17
35. Harlow, E. & Lane, D. (1988) *Antibodies, a Laboratory Manual*, Cold Spring Harbor Laboratory, Cold Spring Harbor, NY
36. Tamiya, T., Lamouroux, A., Julien, J. F., Grima, B., Mallet, J., Fromageot, P. & Ménez, A. (1985) *Biochimie* **67,** 185–189
37. Kunkel, T. A., Roberts, J. D. & Zakour, B. A. (1987) *Methods Enzymol.* **154,** 367–382
38. Kalnins, A., Otto, K., Rüther, U. & Müller-Hill, B. (1983) *EMBO J.* **2,** 593–597
39. Laemmli, U. K. (1970) *Nature* **227,** 680–685
40. Ellman, G. L., Courtney, K. D., Andres, V., Jr. Featherstone, R. M. (1961) *Biochem. Pharmacol.* **7,** 88–95
41. le Du, M. H., Marchot, P., Bougis, P. E. & Fontecilla-Camps, J. C. (1992) *J. Biol. Chem.* **267,** 22122–22130
42. van den Born, H. K. L., Radić, Z., Marchot, P., Taylor, P. & Tsigelny, I. (1995) *Protein Sci.* **4,** 703–715
43. Pillet, L., Trémeau, O., Ducancel, F., Drevet, P., Zinn-Justin, S., Pinkasfeld, S., Boulain, J.-C. & Ménez, A. (1993) *J. Biol. Chem.* **268,** 909–916
44. Trémeau, O., Lemaire, C., Drevet, P., Pinkasfeld, S., Ducancel, F., Boulain, J.-C. & Ménez, A (1995) *J. Biol. Chem.* **270,** 9362–9369
45. Mebs, D. & Claus, I. (1991) in *Snake Toxins* (Harvey, A. L., ed) pp. 425–447, Pergamon Press, New York
46. Ducancel, F., Boulain, J. C., Trémeau, O. & Ménez, A. (1989) *Protein Eng.* **3,** 139–143
47. Boyot, P., Pillet, L., Ducancel, F., Boulain, J. C, Trémeau, O. & Ménez, A. (1990) *FEBS Lett.* **266,** 87–90
48. Fiordalisi, J. J., Fetter, C. H., Ten-Harmsel, A., Gigowski, R., Chiappinelli, V. A. & Grant, G. A. (1991) *Biochemistry* **31,** 10337–10343
49. Fiordalisi, J. J., Al-Rabiee, R., Chiappinelli, V. A. & Grant, G. A. (1994) *Biochemistry* **33,** 3872–3877
50. Fiordalisi, J. J., Al-Rabiee, R., Chiappinelli, V. A. & Grant, G. A. (1994) *Biochemistry* **33,** 12962–12967
51. Rosenthal, J. A., Hsu, S. H., Schneider, D., Gentile, L. N., Messier, N. J., Vaslet, C. A. & Hawrot, E. (1994) *J. Biol. Chem.* **269,** 11178–11185
52. Lu, X., Rahman, S., Kakkar, V. V. & Authi, K. S. (1996) *J. Biol. Chem.* **271,** 289–294
53. Fiordalisi, J. J., James, P. L., Zhang, Y. & Grant, G. A. (1996) *Toxicon* **34,** 213–224
54. Ménez, A. (1991) in *Snake Toxins* (Harvey, A. L., ed) pp. 35–90, Pergamon Press, New York
55. Straus, O. H. & Goldstein, A. (1943) *J. Gen. Physiol.* **26,** 559–585
56. Greco, W. R. & Hakala, M. T. (1979) *J. Biol. Chem.* **254,** 12104–12109
57. Cerveñansky, C., Engström, A. & Karlsson, E. (1995) *Eur. J. Biochem.* **229,** 270–275
58. Barak, D., Kronman, C., Ordentlich, A., Ariel, N., Bromberg, A., Marcus, D., Lazar, A., Velan, B. & Shafferman, A. (1994) *J. Biol. Chem.* **269,** 6296–6305
59. Shafferman, A., Velan, B., Ordentlich, A., Kronman, C., Grosfeld, H., Leitner, M., Flashner, Y., Cohen, S., Barak, D. & Ariel, N. (1992) *EMBO J.* **11,** 3561–3568
60. Gilson, M. K., Straatsma, T. P., McCammon, J. A., Ripoll, D. R., Faerman, C. H., Axelsen, P. H., Silman, I. & Sussman, J. L. (1994) *Science* **263,** 1276–1278
61. Axelsen, P. H., Harel, M., Silman, I. & Sussman, J. L. (1994) *Protein Sci.* **3,** 188–197
62. Le Du, M. H., Housset, D., Marchot, P., Bougis, P. E., Navaza, J. & Fontecilla-Camps, J. C. (1996) *Acta Crystallogr. Sec. D* **52,** 87–92
63. Cerveñansky, C., Engström, A. & Karlsson, E. (1994) *Biochim. Biophys. Acta* **1199,** 1–5
64. Chothia, C. & Janin, J. (1975) *Nature* **256,** 705–708
65. Janin, J. & Chothia, C. (1990) *J. Biol. Chem.* **265,** 16027–16030
66. Padlan, E. A. (1990) *Proteins* **7,** 112–124
67. Jin, L., Fendly, B. M. & Wells, J. A. (1992) *J. Mol. Biol.* **226,** 851–865
68. Nuss, J. N., Bossard Whitaker, P. & Air, G. M. (1993) *Proteins* **15,** 121–132
69. Clackson, T. & Wells, J. A. (1995) *Science* **267,** 383–386
70. Roussel, A. & Cambillau, C. (1989) in *Silicon Graphics Geometry Partners Directory* (Silicon Graphics Committee, eds) pp. 77–78, Mountain View, CA